Complexation of Oppositely Charged Polyelectrolytes: Effect of Ion Pair Formation

Alexander Kudlay,* Alexander V. Ermoshkin,† and Monica Olvera de la Cruz‡

Department of Materials Science and Engineering, Northwestern University, Evanston, Illinois 60208

Received July 19, 2004; Revised Manuscript Received September 10, 2004

ABSTRACT: Complexation in symmetric solutions of oppositely charged polyelectrolytes is studied theoretically. We include polyion cross-linking due to formation of thermoreversible ionic pairs. The electrostatic free energy is calculated within the random phase approximation taking into account the structure of thermoreversible polyion clusters. The degree of ion association is obtained self-consistently from a modified law of mass action, which includes a long-range electrostatic contribution. We analyze the relative importance of the three complexation driving forces: long-range electrostatics, ion association, and van der Waals attraction. The conditions on the parameters of the system that ensure stability of the complex with addition of salt are determined.

I. Introduction

The complexation of oppositely charged polyelectrolytes in different ionic conditions is an interesting problem of biological relevance.[1−4] Moreover, the association of two oppositely charged linear chains has implications in the design of new materials with unique properties such as multilayer polyelectrolytes[5,6] and carrier gels for drug delivery.[7] Industrial applications include uses as coatings, flocculants, and absorbents.[8,9]

Charged chains can associate via many mechanisms given the large number of length scales involved in these mixtures. The properties of the complexes are strongly dependent on physical parameters such as salt and monomer concentrations and on the chemical configurations of the chains such as their charge densities, persistence lengths, degrees of polymerization, and nature of the interactions between the charge groups along the backbone.[10−14]

Complexes formed by chains with low charge densities have been analyzed using linearized models.[15−19] These models are applicable to describe solutions with strongly hydrated charge groups of positive and negative charges, which interact weakly with each other. In these studies, ion condensation effects[20,21] can be neglected if the linear charge density is sufficiently low. As first suggested by Borue and Erukhimovich,[15] the complexation in these systems occurs via collective charge fluctuations.[15−18] With addition of salt, the complexes dissolve due to screening of electrostatic interactions.

In certain polymer mixtures, even when the charge density is low, nonlinear effects are important if the charge groups are strongly interacting. In these mixtures the oppositely charged groups, when placed at short separation distances, can be locally dehydrated, and act as localized short-range cross-links between oppositely charged groups along the chains. The formation of these links generates a thermoreversibly cross-linked solution[22−25] of oppositely charged chains. The number of cross-links formed in equilibrium in such thermoreversibly associating chains is given by the law of mass action with an effective association constant. In uncharged systems the association constant depends exponentially on the strength of the short range attraction between the reactive groups. For charged reactive groups, however, there is an additional term in the association constant due to the electrostatic contribution to the free energy resulting from the collective charge fluctuations. Since association occurs between the ions belonging to oppositely charged chains, this additional electrostatic term always increases the rate of association. The importance of nonlinear association of charges has been recently recognized in polyelectrolyte adsorption[26,27] and multilayer formation.[28]

In this work the electrostatic interactions are described using a two-fold approach. The strongly nonlinear short-range interactions between oppositely charged groups are accounted for by including strong correlations between the chains. The long-range electrostatic interactions (which are weak for weakly charged polyelectrolytes) are accounted for in a linearized way by computing the fluctuations of this correlated solution of cross-linked charged chains using a generalized Debye−Hückel approach (random phase approximation).[29,30] The electrostatic free energy depends on the structure of charged polymer clusters, while the cluster distribution depends (through the modified law of mass action) on the electrostatic free energy. Therefore, we determine here the number of formed cross-links by evaluating self-consistently the electrostatic contribution from the collective charge fluctuations of a cross-linked system of charged chains.

The degree of hydrophobicity of the chain backbone modifies the thermodynamics of the solution.[18] We consider nonselective solvents, where the degree of compatibility is the same for both the positively and negatively charged chains. We investigate how the degree of hydrophobicity influences the properties of complexes formed by electrostatic interactions.

The paper is organized as follows. In section II, we describe the model and approximations used and derive the free energy of the solution; the details of the derivation of the correlation function of the cross-linked system required to determine the electrostatic contribution to the free energy is given in Appendix A. In section

* Corresponding author. E-mail: kudlay@northwestern.edu.
† E-mail: ermosh@email.unc.edu. Present address: Department of Chemistry, University of North Carolina, Chapel Hill, NC, 27599.
‡ E-mail: m-olvera@northwestern.edu.

10.1021/ma048519t CCC: $27.50
Published on Web 10/29/2004

III, we discuss how different system parameters influence the properties of the formed complex and its response to addition of salt. The conclusions are given in section IV.

II. The Free Energy of the Semidilute Solution

A. Model. In this section, we calculate the free energy of a homogeneous semidilute solution of oppositely charged polyelectrolytes. For simplicity in this work we consider only the absolutely symmetric case. Positively and negatively charged chains are present in the solution in equal concentrations and have the same physical properties except for the sign of the charge. The chains have degree of polymerization $N = N_1 = N_2$. The fraction of charged monomers on both types of chains is equal to f. We consider only weakly charged chains for which f is small enough, so that electrostatic energy of adjacent along the chain charges is smaller than the thermal energy.[31,32] The number concentrations of positively and negatively charged monomeric units are $\rho_1 = \rho_2$, so that the total concentration of monomeric units in the solution is $\rho = 2\rho_1/f$. Each charged monomeric unit releases a monovalent counterion. A 1:1 low molecular salt can also be present in the solution with concentration of positively and negatively charged ions given by ρ_{s+} and ρ_{s-}, respectively, and the total concentration of salt ions $\rho_s = 2\rho_{s+} = 2\rho_{s-}$. Since the effect of counterions is equivalent to addition of salt, we include the counterions in the salt.

We describe strong electrostatic interactions between oppositely charged monomeric units as thermoreversible bond (cross-link) formation. This strong nonlinear interaction should be treated differently from the long-range electrostatic part, which is accounted for within the random phase approximation (RPA).[29,30] Another reason formation of ionic pairs should be considered in addition to Coulomb interactions is because formation of ionic pairs can proceed with the rearrangement of the solvation shell of charges on polymer. In this case, the effective dielectric constant between charges in a pair can differ significantly from the bulk solvent dielectric constant. Thus, the bond energy in a pair can be quite high. A natural model to describe such ion-pairing is reversible association between charges of opposite signs. For simplicity we assume that only pairs can be formed, with the absolute value of the reduced bond energy $\epsilon = |E|/kT$ (k is the Boltzmann constant, T the thermodynamic temperature), which gives rise to association constant $\omega = e^{\epsilon}$. Typically, the energy $|E|$ is on the order of several kT.[26−28] Note that bond formation is different from short-range van der Waals attraction in that it has the saturation property; that is, once a bond between two given ions is formed, they do not interact with any other ions.

We write the free energy of the solution of associating polyelectrolytes in the following form

$$F = F_{ref} + F_{RPA} \tag{1}$$

where the first term is the free energy of the reference neutral system (but with short-range interactions) and the second term is the contribution of electrostatics. The electrostatic part F_{RPA} is calculated within the RPA, which is a linear theory equivalent to the Debye−Hückel approximation (i.e., to the linearized Poisson−Boltzmann equation). For the reference free energy, we use the Flory−Huggins mean-field approximation

$$F_{ref} = F_{id} + F_{FH} \tag{2}$$

which includes the ideal entropic and enthalpic terms. In our associating system the ideal term is the free energy of ideal gas of all possible clusters {C} with appropriate statistical weights ω(C)

$$\frac{F_{id}}{kT\mathcal{V}} = \sum_{\{C\}} \rho(C) \ln\frac{\rho(C)}{e\omega(C)} + \rho_{s-} \ln\frac{\rho_{s-}}{e} + \rho_{s+} \ln\frac{\rho_{s+}}{e} \tag{3}$$

as well the entropy of the ideal gas of salt ions (counterions are also included here). As has been shown in refs 23 and 24, the equilibrium concentrations ρ(C) can be obtained using a diagrammatic technique and the free energy of associating chains can be written as

$$\sum_{\{C\}} \rho(C) \ln\frac{\rho(C)}{e\omega(C)} = \frac{\rho}{N}\ln\rho + \rho f\,[(1-\Gamma)\ln(1-\Gamma) + \Gamma\ln\Gamma] - \frac{\rho f\Gamma}{2}\ln\left[\frac{\rho f\Gamma}{2e} v e^{\epsilon}\right] \tag{4}$$

Here conversion Γ is the fraction of polymeric ions in pairs (see Appendix A), which is to be found from subsequent minimization of the total free energy of the solution. The volume of the monomeric unit v (which we for simplicity assume to be equal to $v = b^3$) is used to approximate the internal partition function of the cross-link $Z_{cross} = ve^{\epsilon}$. An alternative combinatorial derivation of (4) can be performed along the lines of ref 33.

We assume that the polycation and polyanion backbones have identical short-range interaction with solvent. The interaction free energy in (2) is assumed to be given by the Flory−Huggins form

$$\frac{F_{FH}}{kT\mathcal{V}/b^3} = (1-\phi-\phi_s)\ln(1-\phi-\phi_s) + \chi\phi(1-\phi) \tag{5}$$

where V is the volume of the system, $\phi = \rho b^3$ is the total polymer volume fraction, and $\phi_s = b^3\rho_s = 2b^3\rho_{s-}$ is the total volume fraction of salt ions (and also counterions). The first term in (5) stems from hardcore repulsion; the second one from short-range attraction, whose strength is characterized by the parameter χ. We will analyze both the cases of good and marginal to bad solvent. Note that, in contrast to previous works,[16,34] interactions of backbones with solvent favor complexation under bad solvent conditions.

Adding up the two contributions, the free energy F_{ref} of the reference neutral system reads

$$\frac{F_{ref}}{kT\mathcal{V}/v} = \frac{\phi}{N}\ln\phi + \phi_s\ln\phi_s + \phi f[(1-\Gamma)\ln(1-\Gamma) + \Gamma\ln\Gamma] - \frac{\phi f\Gamma}{2}\ln\left[\frac{\phi f\Gamma}{2e}e^{\epsilon}\right] + (1-\phi-\phi_s)\ln(1-\phi-\phi_s) + \chi\phi(1-\phi) \tag{6}$$

B. Electrostatic Free Energy: Random Phase Approximation. Because of electroneutrality, the electrostatic contribution F_{RPA} in the total free energy in (1) is due to fluctuations of charge concentrations,[15,29] which is calculated within the random phase approximation (see ref 24 for details):

$$\frac{F_{\mathrm{RPA}}}{kT} = \frac{V}{2}\int \frac{\mathrm{d}^3q}{(2\pi)^3}[\ln(\det(\mathbf{I}+\mathbf{G}(q)\mathbf{U}(q))) - \sum_i \rho_i U_{ii}(q)] \quad (7)$$

Here $\mathbf{I} = ||\delta_{ij}||$ is the unitary matrix, $\mathbf{G}(q)$ is the correlation function matrix of the reference neutral system, and $\mathbf{U}(q)$ is the matrix of Coulomb interactions. The sum runs over all charged components of the system (co-ions and salt ions). The last term in (7) is the self-energy of pointlike charges.

The correlation function matrix $\mathbf{G}(q)$ can be in turn obtained within the RPA as[35−37]

$$\mathbf{G}^{-1}(q) = \mathbf{g}^{-1}(q) + \mathbf{c}(q) \quad (8)$$

where $\mathbf{g}(q)$ is the structure correlation matrix. It characterizes correlations of density due to existence of different clusters in the system, but does not include interactions. The matrix $\mathbf{g}(q)$ for our symmetric system has the form

$$g_{ij} = \begin{pmatrix} g_{11} & g_{12} & 0 & 0 \\ g_{12} & g_{11} & 0 & 0 \\ 0 & 0 & \rho_{s-} & 0 \\ 0 & 0 & 0 & \rho_{s+} \end{pmatrix} \quad (9)$$

Since the RPA correction is due to electrostatic interactions, in its derivation we have to consider only charged monomeric units. Thus, the matrices **G**, **g**, and **c** have only four components corresponding to positively and negatively charged monomeric units and salt ions, while neutral monomers do not enter consideration. The correlation functions g_{11} and g_{12} of charged monomeric units are calculated in Appendix A using a diagrammatic approach. The interaction matrix $\mathbf{c}(q)$ describes short-range interactions (free energy F_{FH}) and its components are given by

$$c_{ij} = \frac{1}{\Phi}s_i s_j - 2\chi p_i p_j \quad (10)$$

where we introduced the volume fraction of solvent $\Phi = 1 - \phi - \phi_s$ and two auxiliary vectors

$$s_i = \{1, 1, 1, 1\} \quad (11)$$

$$p_i = \{1, 1, 0, 0\} \quad (12)$$

Using the vector of valencies e_i, the Coulomb interaction matrix can be written in the following form

$$U_{ij}(q) = e_i e_j U(q) \quad (13)$$

$$e_i = \{1, -1, 1, -1\} \quad (14)$$

which allows us to simplify the expression under the logarithm in (7)

$$\det(\mathbf{I}+\mathbf{G}(q)\mathbf{U}(q)) = 1 + U(q)\sum_{i,j} G_{ij}(q) e_i e_j \quad (15)$$

Using formulas 10 and 12 for the correlation functions g_{ij} and c_{ij}, we now can obtain G_{ij} in accordance with (9). Substituting the result into (15) we finally obtain

$$\det(\mathbf{I}+\mathbf{G}(q)\mathbf{U}(q)) = 1 + U(q)\{2g_{11} - 2g_{12} + 2\rho_{s-}\} \quad (16)$$

It is remarkable that this result is the same as if we had neglected the short-range interactions (the matrix c_{ij}), that is, if we had put $G_{ij} = g_{ij}$ in determinant 15. The independence of the electrostatic RPA contribution on short-range interactions was already noticed in ref 15. Note, however, that this simple result holds only for our case of a symmetric system (described by matrix g_{ij}) and for symmetric long-range (matrix $\mathbf{U}(q)$) and short-range (matrix **c**) interactions.

The structure correlation functions g_{ij} are calculated in Appendix A (see eqs A20 and A21). We reproduce them here for convenience

$$g_{11}(q) = \rho_1 g(q)\frac{1 + (\Gamma')^2 h(q)}{1 - [\Gamma' h(q)]^2} \quad (17)$$

$$g_{12}(q) = \rho_1 g(q)\frac{\Gamma' g(q)}{1 - [\Gamma' h(q)]^2} \quad (18)$$

The functions $g(q)$ and $h(q)$ are defined by (A6) and (A9) in Appendix A. The effective conversion Γ' is defined as $\Gamma e^{-q^2b^2/6}$ in (A19), with the bare conversion Γ defined as the fraction of charged monomers participating in cross-links (see eq A15). It is important to note that the correlation functions (eqs 17 and 18) are calculated for an ideal thermoreversibly associating system, in which no other interactions except cross-linking are present (in our case no electrostatic and hydrophobic interactions).[24]

Substituting these expressions into (16) we can rewrite the free energy in (7) as

$$\frac{F_{\mathrm{RPA}}}{kT} = \frac{V}{2}\int \frac{\mathrm{d}^3q}{(2\pi)^3}\left[\ln\left(1 + U(q)\left\{\rho f g(q)\frac{1-\Gamma'}{1+\Gamma' h(q)} + \rho_s\right\}\right) - \sum_i \rho_i U_{ii}(q)\right] \quad (19)$$

where $\rho f = 2\rho_1 = 2\rho_2$ and $\rho_s = 2\rho_{s-} = 2\rho_{s+}$.

To be able to evaluate F_{RPA} we need to specify a suitable form of the interaction potential $U(q)$. For the bare Coulomb interaction, we have

$$\frac{U_C(r)}{kT} = \frac{{q_e}^2}{\epsilon kT b}\frac{1}{r} = \frac{l}{r} \quad (20)$$

$$\frac{U_C(q)}{kT} = \int \mathrm{d}^3r\, \mathrm{e}^{i\mathbf{qr}} U_C(r) = \frac{4\pi l}{q^2} \quad (21)$$

Here we introduced the reduced Bjerrum length $l \equiv l_B/b$, $l_B = {q_e}^2/(\epsilon kT)$, where q_e is the electron charge and ϵ the dielectric constant of the solvent. In water $\epsilon \approx 80$, which leads to $l_B \approx 7$Å. To take into account the influence of the hardcore of the ions on the electrostatic contribution F_{RPA}, we used a modified Coulomb potential given by

$$\frac{U(r)}{kT} = \frac{l}{r}(1 - \mathrm{e}^{-r/b}) \quad (22)$$

$$\frac{U(q)}{kT} = \frac{4\pi l}{q^2(1+q^2b^2)} \quad (23)$$

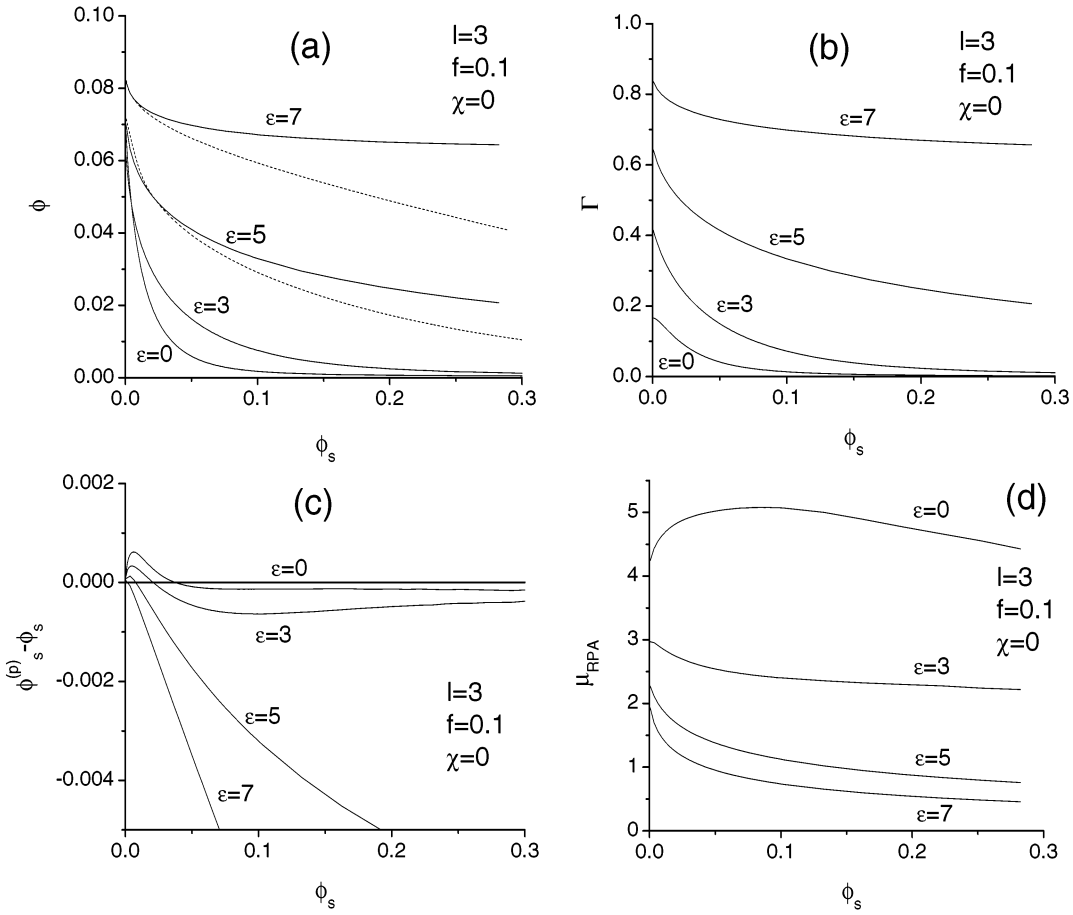

Figure 1. (a) Polymer volume fraction in the precipitate ϕ as a function of the salt volume fraction in the supernatant ϕ_s for different binding energies ϵ. Dashed lines correspond to the assumption of equality of salt concentrations in the precipitate and supernatant: $\phi_s^{(p)} = \phi_s$. (b) Conversion Γ for curves of plot a. (c) Difference of salt volume fractions in the precipitate and supernatant $\phi_s^{(p)} - \phi_s$ for the curves of plot a. (d) Electrostatic binding energy μ_{RPA} in the precipitate.

where we for simplicity assumed that the size of the ions in equal to the bond length b. This is a good assumption for flexible chains, such as NaPSS ($b \approx 2.5$ Å) with added NaCl (hydrated ion radii ≈ 3.5 Å). At large distances ($r \gg b$) the modified potential becomes the pure Coulomb potential (eqs 20 and 21). However, at $r = 0$, the modified potential attains a finite value, while the original Coulomb potential diverges. Thus, we phenomenologically include the impenetrability of the ions within the RPA formalism, which is originally formulated for pointlike ions. The RPA with the modified potential (eqs 22 and 23) has been shown to successfully describe the phase diagrams of polyelectrolytes[38] and of the low-molecular system of charged dumbbells.[39] Furthermore, this potential has been successfully used in the liquid-state approaches.[40] Note that there are two limitations to the Debye−Hückel description of pointlike ions: (1) at the concentration when the size of the ions becomes important one cannot neglect the impenetrability of the ions; (2) when the electrostatic interactions become stronger than the thermal energy one cannot neglect the effects of ion pairing. As we showed in ref 39, when both effects are incorporated in the RPA description the resulting theory yields good quantitative description of simple electrolytes beyond the Debye−Hückel limit. In the present work we incorporate the effects of ion size by using the potential (eqs 22 and 23), but neglect the ion paring of salt ions. The linear character of interactions breaks down at $(4\pi l \rho_s)^{1/2} l \sim 1$, which for our case of $l = 3$ is at a rather small volume fraction $\phi_s \sim 0.003$ (such an estimation neglects important numerical prefactors which can be large). Therefore, the salt concentrations of interest lie beyond the limit of the Debye−Hückel theory. Since we neglect ion pairing at high concentrations, but include ion impenetrability (as was shown in refs 38 and 39), we expect our description of salt to be only semiquantitatively correct at very high salt concentrations (see also the discussion of Figure 1d). Note that consistent with the results in simple liquids,[39,40] inclusion of the impenetrability of the ions is essential to avoid unphysical features at very high salt concentrations.

Substituting the modified potential (23) into (19), we obtain the final expression for the electrostatic free energy

$$\frac{F_{RPA}}{kT} = \frac{V}{2}\int \frac{d^3q}{(2\pi)^3}\left[\ln\left(1 + \frac{4\pi l}{q^2(1+q^2b^2)}\left\{\rho f g(q)\frac{1-\Gamma'}{1+\Gamma' h(q)} + \rho_s\right\}\right) - \frac{4\pi l}{q^2(1+q^2b^2)}(\rho f + \rho_s)\right] \quad (24)$$

Let us make several comments on the structure of F_{RPA}. The polymer structure correlation functions (eqs 17−23) diverge at the gelation condition $\Gamma(Nf - 1) = 1$, which is simply due to the fact that gelation corresponds to the formation of an infinite cluster. It is remarkable

that the electrostatic free energy (eq 24) has no corresponding singularity at the gelation structural transition. This is due to the charge symmetry of the considered system. Indeed since in our case association is possible only between oppositely charged chains (which carry the same amount of charge) the infinite cluster is by construction neutral, therefore does not contribute to F_{RPA}. (It can be shown that for any asymmetric system (asymmetry of N, ρ, or f) the infinite cluster is charged, and accordingly, the expression for F_{RPA} has a singularity at and beyond the gelation transition. However, this unphysical singularity is an artifact of our simplified description of gel structure.)

Let us look at the limiting cases of eq 24. By putting $\Gamma' = 0$, we regain the well-known expression for free unassociated chains, and if we put $\Gamma' = 1$, the polyelectrolyte chains do not contribute to F_{RPA}. However, since Γ' is only the effective conversion: $\Gamma' = \Gamma e^{-q^2b^2/6}$ the equality $\Gamma' = 1$ is possible only when $\Gamma = 1$ and $q = 0$. On all finite length scales ($q \neq 0$) charges in cross-links still contribute to the electrostatic free energy F_{RPA}. This is natural, since in our model of cross-linking the two opposite charges do not annihilate; instead, they are considered as separate charges with Gaussian correlations between them, which leads to the emergence of effective conversion Γ', instead of bare conversion Γ. Because the charges do not annihilate when the ionic pairs are formed, we subtract the self-energy of all ions present in the system (last term in (24)), regardless of whether they are free or form cross-links.

The chain correlation functions $g(q)$ and $h(q)$ are defined by (A6) and (A9). The function $g(q)$ can be easily calculated in the continuous limit, the result being the well-known Debye structure−function. However, we also need the correct limit of pointlike ions at $q \to \infty$ in (24), since we subtract the self-energy of all ions. Therefore, we choose a simple interpolation form for the chain structure−function $g(q)$

$$g(q) = 1 + \frac{Nf}{1 + q^2b^2N/12} \tag{25}$$

$$h(q) = g(q) - 1 \tag{26}$$

which gives the correct limit at $q = 0$, has the scaling of a Gaussian chain at $N^{1-/2} \ll qb \ll f^{1/2}$, and reproduces pointlike ions at $qb \gg f^{1/2}$.

Strictly speaking, the random phase approximation is known to be valid only at sufficiently high polymer concentrations where the chain conformations and electrostatic interactions are decoupled.[29] For solution of polyelectrolyte chains of one sign the approach is strictly applicable only when the electrostatic blobs[31] begin to overlap, which can be shown to occur at $\phi \sim (lf^2)^{1/3}$. For typical values $l = 3$ and $f = 0.1$ (corresponds to highly flexible weakly charged polyelectrolytes in water) this gives a rather high value of $\phi \sim 0.17$. For our case of symmetric solution of oppositely charged chains this is only a rough upper estimate, since when oppositely charged chains cross-link locally the chains neutralize each other, so that there is no influence of electrostatics at much lower concentrations than $\phi \sim (lf^2)^{1/3}$. To account for existence of electrostatic blobs one needs to modify the chain structure factor (for example, as it was done in ref 24) or use an appropriate scaling approach (see ref 25). However, such a modification leads only to insignificant quantitative corrections, therefore in this work for simplicity we use Gaussian statistics for all length scales.

C. Minimization of the Free Energy. The total free energy (eq 1) is given by the sum of F_{ref} in (6) and F_{RPA} in (24). However, this is only the virtual free energy of a system with a given value of conversion Γ. To obtain the equilibrium free energy $F(\Gamma_{eq})$ we need to obtain the equilibrium conversion Γ_{eq}, by the minimization of $F(\Gamma)$:

$$\frac{\partial F(\Gamma)}{\partial \Gamma} = 0 \tag{27}$$

Using (6) and (24), we obtain the following equation for Γ

$$\frac{\Gamma}{(1-\Gamma)^2} = \frac{\phi f}{2}\exp[\epsilon + \mu_{RPA}(\Gamma)] \tag{28}$$

This equation has the general structure of the law of mass action. A noteworthy feature of (28), however, is that the energy gained from formation of a cross-link consists of the bonding energy ϵ and the energy gain μ_{RPA}, a chemical-potential-like quantity defined as

$$\mu_{RPA}(\Gamma) = \frac{\partial F_{RPA}(\Gamma)}{\partial \Gamma}\left(\frac{\rho f}{2}\right)^{-1} \tag{29}$$

which results from the long-range electrostatic attraction of the polymer chains described by F_{RPA}. Using eq 24, we obtain

$$\mu_{RPA}(\Gamma) = \int \frac{d^3q}{(2\pi)^3}\frac{U(q)}{1 + U(q)K(q)}\frac{g^2(q)e^{-q^2b^2/6}}{[1 + \Gamma' h(q)]^2} \tag{30}$$

$$U(q) = \frac{4\pi l}{q^2}\frac{1}{1 + q^2a^2} \tag{31}$$

$$K(q) = \rho f g(q)\frac{1 - \Gamma'}{1 + \Gamma' h(q)} + \rho_s \tag{32}$$

Of course, the energy μ_{RPA} depends on the thermodynamic state of the solution, and thus on Γ; therefore, eqs 28 and 30 are to be solved simultaneously to obtain $\Gamma(\phi)$. Since in our model cross-linking takes place only between oppositely charged chains $\mu_{RPA}(\Gamma)$ is always positive, that is, the electrostatic attraction, along with the specific binding energy ϵ, always promotes cross-linking. From the numerical solution one obtains that $\mu_{RPA}(\Gamma)$ is a monotonically decreasing function of Γ for all ϕ, which is explained by the fact that as more ions associate they contribute less to the long-range attraction (which can be seen directly from F_{RPA} in (24)).

III. Results and Discussion

Because of its complete symmetry, only macroscopic phase separation is possible in the considered system. In our ternary incompressible system of polymer, salt and solvent, we have two independent components, which we choose to be polymer and salt. When macroscopic phase separation (precipitation) occurs, the two coexisting phases differ in concentrations of both polymer and salt. Thus, generally speaking, we have to calculate the phase diagrams of a ternary incompressible system. However, we are mostly interested in two aspects of the precipitation process: the influence of different competing complexation mechanisms on the density of the formed precipitate (studied in the next

section) and determination of the conditions of solubility of the complexes with addition of salt (section III.B). In both of these cases, we can make specific additional assumptions which allow us to investigate the mentioned problems in a simple and clear manner.

A. Density of Precipitate: Effect of Cross-Linking and van der Waals Attraction. In our model, we consider three complexation driving forces: long-range electrostatic attraction between co-ions, strongly nonlinear short-range attraction leading to ion-cross-linking, and van der Waals attraction between all monomeric units. In this section, we look at the density of the formed complex ϕ, in particular how ϕ depends on the relative importance of the three complexation factors as well as how the density is influenced by the addition of salt. We can significantly simplify the analysis if we make the following two assumptions (similar to the ones employed in our previous work).[18] First, we assume an infinite degree of polymerization $N = \infty$. Second, the total concentration of polymer chains in the whole solution (system) is assumed to be small. Since the entropy of the chains represents the only driving force for dissolution of the polymer chains from the precipitate, the first assumption amounts to assuming zero polymer concentration in the supernatant (which for a finite N would be a polymer-poor phase). The second assumption is equivalent to assuming that the salt volume fraction in the supernatant is equal to the salt volume fraction in the whole system, which we thus denote simply as ϕ_s. Note that the salt volume fraction in the precipitate $\phi_s^{(p)}$ can differ considerably from ϕ_s, which, as we show below, has a significant effect on ϕ. Given our assumptions, ϕ and $\phi_s^{(p)}$ can be found by equating the pressure and the chemical potential of the salt in the coexisting phases:

$$p(\phi = 0, \phi_s) = p(\phi, \phi_s^{(p)}) \tag{33}$$

$$\mu_s(\phi = 0, \phi_s) = \mu_s(\phi, \phi_s^{(p)}) \tag{34}$$

$$\mu_s = \frac{\partial \mathscr{F}}{\partial \phi_s} \tag{35}$$

$$p = -\mathscr{F} + \sum_{i=1}^{2} \phi_i \frac{\partial \mathscr{F}(\{\phi_i\})}{\partial \phi_i} \tag{36}$$

For convenience here and in the following we use a dimensionless equilibrium free energy density defined by $\mathscr{F} = F(\Gamma_{eq})/(kTV/v)$. The equilibrium free energy $F(\Gamma_{eq})$ is obtained from the minimization (described in section IIC) of the total free energy, which according to (1) is given by the sum of (6) and (24). Similar assumptions were made in the work of Borue and Erukhimovich,[15] except that they additionally assumed the difference $\phi_s^{(p)} - \phi$ to be small. We solve eqs 33 and 34 numerically to obtain ϕ and $\phi_s^{(p)}$, considering ϕ_s as a parameter. The results are given in Figures 1–3.

In Figure 1, we assume no van der Waals attraction $\chi = 0$ and plot results for varying bonding energy $\epsilon = E/kT$. (Experiments on polyelectrolyte adsorption[26,27] and multilayer formation[28] are consistent with the value of binding energy ϵ varying between $\epsilon = 3$ and $\epsilon = 7$.) We set the dimensionless Bjerrum length $l = 3$, which approximately corresponds to aqueous solutions ($l_B \approx 7$Å) of flexible chains (such as NaPSS $b \approx 2.5$Å). The fraction of charged monomers is $f = 0.1$. The dependence

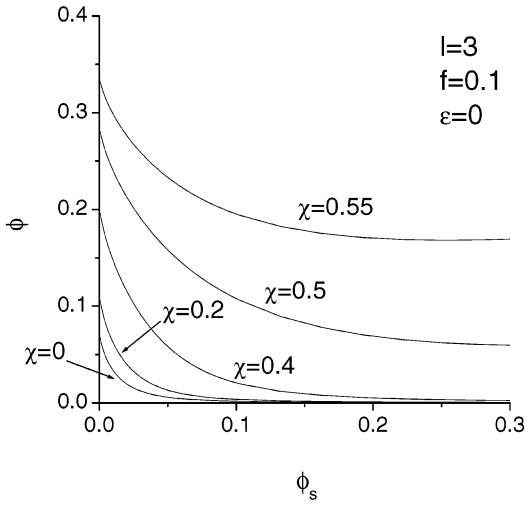

Figure 2. Effect of the Flory–Huggins χ-parameter on the change of polymer volume fraction in the precipitate ϕ with increasing salt in the system ϕ_s.

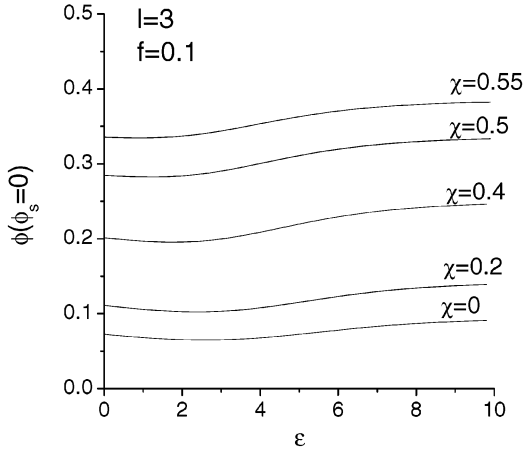

Figure 3. Variation of the density of the precipitate for salt-free system with changing binding energy ϵ. Different curves correspond to different values of the χ-parameter.

of ϕ on l and f for the case of complexation without cross-linking was investigated in our previous work.[18] Similar to the results for that case, ϕ increases with increasing l and/or f for all ϕ_s, ϵ, or χ. With good precision, one can obtain results for other values of f simply by linearly scaling ϕ with f. In the following figures, we plot results for rather high salt concentrations of up to $\phi_s = 0.3$. This is done with the purpose to demonstrate the theoretical limits of the developed theory for very high salt conditions. At such high salt concentrations atomistic details of interactions between salt ions and solvent molecules become important.

Figure 1a shows the polymer volume fraction in the precipitate ϕ as a function of the salt volume fraction in the system ϕ_s. We see that for all values of ϵ the complex density monotonically decreases with increasing salt concentration. These results agree with those previously obtained by Borue and Erukhimovich[15] for complexation without cross-linking, the situation corresponding in our analysis to small ϵ. The decrease of density is of course due to Debye–Hückel screening by salt, which makes the electrostatic attraction weaker (the term F_{RPA} in the total free energy).

In Figure 1b we plot conversion Γ for curves of plot Figure 1a. We see that conversion also monotonically drops when more salt is added to the system, the

behavior being similar for all values of ϵ. With the increase of ϵ, conversion Γ increases for all salt concentrations. However this does not directly translate into a denser complex as we can see from Figure 1a. Indeed for $\phi_s \approx 0$, we see that ϕ depends nonmonotonically on ϵ, the feature which will be explored in detail in Figure 3. For large salt concentrations the density ϕ is larger for greater ϵ, which is obviously due to increased cross-linking of chains. The presence of cross-links manifests itself in a feeble dependence of ϕ on ϕ_s for larger values of ϵ, which indicates indissolubility by salt of complexes formed primarily by specific short-range attractions. At the same time for small binding energies (such as $\epsilon = 0$ and $\epsilon = 3$) in Figure 1a the density ϕ drops rather abruptly and becomes very small, which indicates dissolution of the complex with addition of salt (this problem will be studied in the next section).

The difference between the salt concentration in the precipitate $\phi_s^{(p)}$and that in the supernatant ϕ_s (which, according to our assumption, is equal to the salt concentration in the whole system) is presented in Figure 1c. We see that for small ϵ the precipitate is first enriched with salt, which (as we showed previously[18]) is due to correlational Debye−Hückel attraction. For small ϵ with increasing salt concentrations $\phi_s^{(p)}$ becomes smaller than ϕ_s and then, as the complex becomes very diluted for large ϕ_s, there is only a negligible difference. For large ϵ we have $\phi_s^{(p)} < \phi_s$ for all salt concentrations. (Note that we plot the difference $\phi_s^{(p)} - \phi_s$ in Figure 1c, of course $\phi_s^{(p)}$ increases with ϕ_s.) The depletion of salt in the precipitate turns out to have a considerable effect on ϕ. In Figure 1a, we plot with dashed lines the curves for $\epsilon = 5$ and $\epsilon = 7$ obtained from eq 33 with the assumption $\phi_s^{(p)} = \phi_s$. The effect can be seen to be especially substantial for larger values of ϕ_s. The depletion was shown in our previous paper[18] to be due to hardcore interactions. It was not observed in the earlier studies of complexation,[15−17] in which the hardcore interactions of the salt ions were not considered. The strength of the effect depends on the ratio of excluded volumes of the monomeric units and salt ions. Our results are obtained under the assumption of equality of these volumes, which is a good approximation for an aqueous solution of flexible chains with added NaCl (for example, the repeat unit of NaPSS is approximately 2.5 Å) and the hydrated radii of Na^+ and Cl^- ions are both approximately 3.5 Å).

In Figure 1d we further characterize the complexes formed at a given ϕ_s by plotting the electrostatic binding energy μ_{RPA}, which along with ϵ promotes pair-formation in the precipitate. First, we note that μ_{RPA} has significant values of the same magnitude as ϵ, which is an indication of strong electrostatic interactions in a pair (indeed $l = l_B/b = 3$). The value μ_{RPA} is larger when few cross-links are formed (smaller ϵ), so that free polymer charges gives rise to a significant long-range contribution. With the addition of salt, μ_{RPA} decreases when ϵ is not very small. This decrease is obviously due to screening by salt. However, for $\epsilon = 0$ (negligible cross-linking due to short-range attraction), μ_{RPA} rather surprisingly initially increases with increasing ϕ_s. For larger ϕ_s screening becomes important and μ_{RPA} decreases for $\epsilon = 0$ also. It should be noted that for large ϕ_s, we expect no dependence of μ_{RPA} on ϵ since charges on the chains are strongly screened by salt. The fact that in Figure 1d μ_{RPA} exhibits this dependence is an artifact of our linearized description of salt in the region where not only impenetrability, but also pair-formation of salt ions should be taken into account. A microscopic description of salt is necessary to describe precipitation even qualitatively at very high salt concentrations. For example, if pure Coulomb potential (instead of eq 23) were used, then we obtain an unphysical increase of ϕ at $\phi_s \gtrsim 0.2$.

In Figure 2, we illustrate the effect of the χ-parameter for the case when the effect of association is small ($\epsilon = 0$). The complex is seen to become denser with increasing short-range attraction for all values of ϕ_s. For $\chi < 0.5$ (good solvent) the volume fraction ϕ strongly decreases with increasing salt (which is an indication of dissolution of the complex for finite N). However, for $\chi \geq 0.5$ (bad solvent condition), the density is seen to be negligibly dependent on ϕ_s for large ϕ_s, with the complex being stable with respect to addition of salt. Comparing Figures 1a and 2, we observe that behavior of ϕ with increasing ϕ_s is qualitatively the same when the complex is formed by cross-linking (ϵ) or van der Waals interactions (χ). Note that we analyze here only marginally bad solvent conditions, for which we can disregard the possibility of necklace formation.[41]

The relative strength of the long-range electrostatic attraction vs cross-linking is demonstrated in Figure 3. We plot the precipitate density ϕ in the salt-free solution as a function of bond energy ϵ. Different curves correspond to varying χ, which spans good to marginal solvent conditions. Increasing ϵ means that a greater number of charges form cross-links. Indeed from the numerical solution we obtain that in all cases Γ monotonically increases with growing ϵ. Thus, increasing ϵ physically means changing the driving force of complexation from long-range charge correlation to cross-linking attraction (numerically, at $\epsilon = 10$ the conversion $\Gamma \approx 1$). Interestingly, as we see from Figure 3, the density ϕ (although it exhibits a shallow minimum as a function of ϵ) is rather insensitive to the value of ϵ. Thus, ion-pairing and long-range correlations lead to polyelectrolyte complexes of similar density, and the two mechanisms can be difficult to distinguish experimentally for salt-free systems. Curves for different χ show qualitatively the same behavior, with ϕ increasing as the solvent worsens.

B. Phase Diagram: Dissolution with Addition of Salt. As can be seen from Figures 1a and 2 for small ϵ and/or χ the density ϕ becomes very small with addition of enough salt, which is indicative of precipitate dissolution for a finite N. In the previous section, we assumed $N = \infty$, so the precipitate never dissolved. In this section, we relax this assumption and look at the phase coexistence.

Let us first investigate the effect of N on the phase coexistence. To simplify the presentation let us assume that the salt volume fractions in the polymer-rich and polymer-poor phases are the same. Thus, we treat ϕ_s as a parameter and obtain the coexisting polymer concentrations by constructing a common tangent to the equilibrium free energy density $\mathcal{F}$. An example of resulting phase diagrams for varying N is shown in Figure 4 (the values of all parameters are given in the plot). The area below the coexistence line (for a given N) corresponds to phase separation (complexation at low salt concentrations), above—to a homogeneous solution (the precipitate dissolves at high salt ϕ_s). Owing to our simplifying assumption of equal ϕ_s in the two phases,

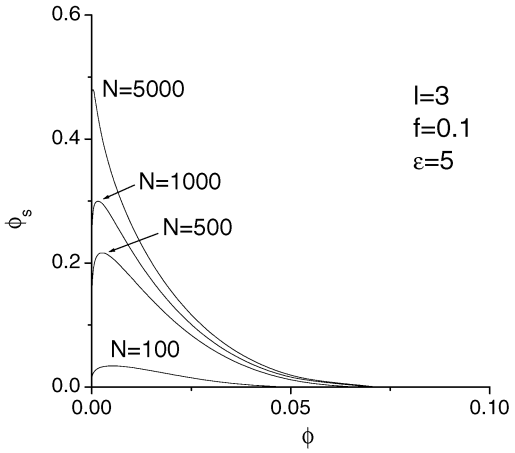

Figure 4. Coexistence lines for phases with different polymer volume fractions ϕ at a given salt volume fraction ϕ_s. The effect of varying chain length N is illustrated.

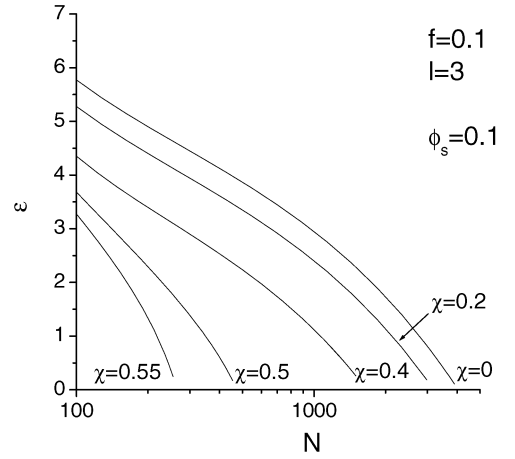

Figure 5. Stability of the precipitate to addition of salt. For all values of the bond energy ϵ and the chain length N below the curve for a corresponding χ value, the precipitate dissolves when the salt concentration is increased beyond $\phi_s > 0.1$.

the tie lines giving the coexisting polymer concentrations are parallel to the ϕ axis. We see that the dilute phase has negligible polymer concentration even for rather small N, which justifies the assumption $N = \infty$ of the previous section. When enough salt is added to the solution the precipitate dissolves. As we can see from Figure 4, the salt concentration needed to dissolve the precipitate strongly depends on N and (as Figures 1 and 2 show) it also depends on ϵ and χ. Similar results were recently obtained experimentally by Kabanov.[42]

In Figure 5, we determine the conditions on ϵ, χ, and N, ensuring stability of the precipitate at a given concentration of salt. For each curve (corresponding to a certain χ) the precipitate exists at $\phi_s = 0.1$ if the values of ϵ and χ lie in the area above the curve, and the precipitate is dissolved in the area below the curve. (The value $\phi_s = 0.1$ is taken as an example, and it applies to all curves.) The increase of either ϵ, χ, or N stabilizes the complex to addition of salt. We observe that the stability of the precipitate is quite sensitive to the values of parameters in the experimentally most relevant region $\epsilon \approx 3$, $\chi \approx 0.5$, and $100 < N < 1000$. The results of Figure 5 can be used for experimental design of complexes stable to salt.

We obtained Figure 5 by considering the spinodal stability of our two component system. The spinodal points are found from the following equation

$$J(\phi,\phi_s) = \begin{vmatrix} \dfrac{\partial^2 \mathscr{F}}{\partial \phi^2} & \dfrac{\partial^2 \mathscr{F}}{\partial \phi \partial \phi_s} \\ \dfrac{\partial^2 \mathscr{F}}{\partial \phi \partial \phi_s} & \dfrac{\partial^2 \mathscr{F}}{\partial {\phi_s}^2} \end{vmatrix} = 0 \qquad (37)$$

with $\mathscr{F} = F(\Gamma_{eq})v/(kT\mathrm{V})$ being the reduced equilibrium free energy. In Figure 5 in the area above the curve for a certain χ the equation $J(\phi,\phi_s = 0.1) = 0$ has two solutions, while in the area below the curve it has no solutions for physical values of ϕ. It should be noted that in our two component system this condition on the existence of spinodal at a given salt is strictly speaking not equivalent to existence of phase separation (to demand that the critical point be at $\phi_s = 0.1$ is yet another different condition). However, in the considered system dissolution occurs at very low ϕ, so the three conditions yield numerically close results.

IV. Conclusions

Complexation in solutions of oppositely charged polyelectrolytes can be accompanied by thermoreversible cross-linking of oppositely charged monomeric ions. A local electrostatic binding energy can exist between oppositely charged units when they tend to be dehydrated in the vicinity of each other or due to nonclassical specific interactions. In this work, we have investigated how the three different mechanisms (long-range electrostatics, cross-linking, and backbone hydrophobicity) define the properties of polyelectrolyte complexes at different salt concentrations.

In our approach, we obtain self-consistently the fraction of cross-linked charged monomers (conversion) and the Debye−Hückel collective fluctuations contribution to the free energy (which depends on conversion). Accordingly, the degree of conversion is determined both by the local binding energy and by long-range electrostatics. We find that the long-range charge fluctuations always promote cross-linking. Given that the magnitude of the Debye−Hückel contribution decreases with increasing salt, the fraction of cross-linked monomers also monotonically decreases with increasing salt.

The polymer concentration in the precipitate is largest at low salt concentration, when the screening of interactions between monomeric ions is weakest. The complex concentration generally decreases monotonically with increasing salt concentration. The rate of complex dilution with addition of salt and the concentration of monomers in the precipitate at high salt are strongly dependent on the value of the van der Waals attractions and on the binding energy. Nonselective net van der Waals attraction between the monomers of both positively and negatively charged chains enhances the complexation in a way broadly similar to cross-linking due to local binding energy. The dilution is very rapid and the monomer concentration of the complex goes to zero in the case of zero binding energy and zero net van der Waals attraction (good solvent condition). Instead, for large values of either type of the short-range attractions, as the salt concentration increases the monomer concentration in the complex generally nearly saturates to a nonzero constant value (or slightly increases for sufficiently large χ). Our results are consistent with experimental observations[43−46] in which, depending on the type of polymers used, with the addition of salt the

complexes can either dissolve or their densities can remain stable. In some cases, initial dissolution and subsequent re-entrant precipitation is observed,[12] the type of behavior obtained in our theory for marginal solvent.

There is an important competition between complexation due to charge fluctuations and nonlinear thermoreversible linking, which is especially interesting under good solvent conditions. Unassociated charged monomeric groups induce complexation due to long-range electrostatics. However, once they form cross-links, they practically do not contribute to long-range attraction. Therefore, at high conversion rates, complexation is mostly due to effective cross-linking attraction in an effectively neutral polymer solution. This competition leads to an interesting nonmonotonic behavior of monomer concentration in the precipitate with increasing the nonlinear binding energy in the case of zero salt concentration: with increasing binding energy the monomer concentration in the precipitate passes through a minimum. Remarkably, the variation in the complex density is rather small; that is, cross-linking and long-range electrostatic attractions give rise to complexes of similar density.

Another important effect in polyelectrolyte complexation is the difference in salt concentrations inside and outside the precipitate. When the nonlinear binding energy is small the difference in salt concentration in and out of the precipitate is negligible. However, for large binding energies (or large values of χ), this difference rapidly grows as the overall salt concentration increases, the precipitate being depleted of salt due to increasing importance of hardcore interactions.[18] We find that for large binding energies and/or in a bad solvent the difference between salt concentrations in the complex and in the bulk has a significant effect on the density of the complex at high salt concentrations. An interesting limit to analyze includes the addition of nonlinear correlations among the ion pairs when the fraction of charged units increases as in the case of strongly charged chains in oppositely charged multivalent ion solution[47,48] where even denser precipitates are expected.

Acknowledgment. This work was supported by NSF Grant DMR 041446. A.V.E. acknowledges partial financial support of NSF Grant EECO 118025.

Appendix A. Calculation of the Structural Correlation Functions

In this section, we calculate the structural correlation functions of the solution of associating oppositely charged polyelectrolytes. Charged groups on chains are treated as stickers that can associate with ionic groups of an opposite sign. We consider only the symmetric case of oppositely charged homopolymers of equal degree of polymerization $N = N_1 = N_2$ (indices 1 and 2 refer to positively and negatively charged chains, respectively). Only the fraction f of monomers is charged, so the number of charges on chains of both types is Nf. Total concentration of monomers of both types is ρ; therefore, the number concentrations of positively and negatively charged monomers are $\rho_1 = \rho_2 = \rho f/2$. We also assume that the chains have the same chemical structure, that is the same bond length $b = b_1 = b_2$ and the distance between charges $a = bf^{-1/2}$. We assume Gaussian statistics for all chains. The expression for the structural correlation function (eq 9) between two different types of monomers α and β reads (for detailed derivation see ref 24)

$$g_{\alpha\beta}(q) = \sum_C \rho(\mathrm{C}) g^{\mathrm{C}}_{\alpha\beta}(q) \tag{A1}$$

$$g^{\mathrm{C}}_{\alpha\beta}(q) = \sum_{i,j} \langle \mathrm{e}^{i\mathbf{q}(\mathbf{r}_i^\alpha - \mathbf{r}_j^\beta)} \rangle_C \tag{A2}$$

Summation in (A1) is over all topologically different clusters formed due to association of polymers, with $\rho(\mathrm{C})$ being the number concentration of a cluster having structure C and $g^{\mathrm{C}}_{\alpha\beta}(q)$ the molecular structural correlation function. In (A2), the summation runs over all monomers of types α and β of the cluster C. The average is over the conformations of the cluster, it can be written as

$$\langle \mathrm{e}^{i\mathbf{q}(\mathbf{r}_i^\alpha - \mathbf{r}_j^\beta)} \rangle_{\mathrm{C}} = \frac{\int \mathrm{e}^{i\mathbf{q}(\mathbf{r}_i^\alpha - \mathbf{r}_j^\beta)} f_{\mathrm{C}}(\Gamma_{\mathrm{C}})\, \mathrm{d}\mathbf{\Gamma}_{\mathrm{C}}}{\int f_{\mathrm{C}}(\Gamma_{\mathrm{C}})\, \mathrm{d}\mathbf{\Gamma}_{\mathrm{C}}} = \frac{1}{V} \int \mathrm{e}^{i\mathbf{q}(\mathbf{r}_i^\alpha - \mathbf{r}_j^\beta)} f_{\mathrm{C}}(\Gamma_{\mathrm{C}})\, \mathrm{d}\mathbf{\Gamma}_{\mathrm{C}} \tag{A3}$$

where $f_{\mathrm{C}}(\Gamma_{\mathrm{C}})$ is the probability function of finding the cluster in conformation Γ_{C}, and the integration is over the entire configurational space of the cluster C.

To calculate the correlation functions (eq A1), we employ the grand canonical diagrammatic technique, first developed in ref 49 for description of weak gels. (For details of the diagrammatic technique as well as applications to other related systems see refs 23, 24, and 50.) Here we generally follow the description provided in ref we. As is shown there, the correlation function can be expressed as the sum of all two-root diagrams

$$g_{\alpha\beta}(q) = \sum_n z^n \sum_{C_n^{\alpha\beta}} \frac{W(C_n^{\alpha\beta})}{S(C_n^{\alpha\beta})} \langle \mathrm{e}^{i\mathbf{q}(\mathbf{r}_i^\alpha - \mathbf{r}_j^\beta)} \rangle_{C_n^{\alpha\beta}} \tag{A4}$$

where z is the fugacity of the chain ($z = \exp(-\mu/kT)$, μ is the chemical potential), $W(\mathrm{C}_n^{\alpha\beta})$ is the statistical weight of the cluster $\mathrm{C}_n^{\alpha\beta}$ with two marked monomers of types α and β, and $S(\mathrm{C}_n^{\alpha\beta})$ is its symmetry index.

To calculate $g_{\alpha\beta}(q)$, it is convenient to introduce the following generating functions. Let us introduce the generating function of all one-root diagrams t (diagrams with one marked monomer), which can be calculated recursively as

$$t = 1 + \omega z t^{fN-1} \frac{fN}{2} \tag{A5}$$

Here ω is the statistical weight of the cross-link: $\omega = \exp(\epsilon)$, where ϵ is the absolute value of the dimensionless cross-link bond energy $\epsilon = |E|/kT$. Now we can write the sum of all labeled diagrams with two labels belonging to the same chain as

$$\Sigma_{\mathrm{g}}(q) = z t^{fN-2} \frac{1}{2} \sum_{i,j} \langle \mathrm{e}^{i\mathbf{q}(\mathbf{r}_i - \mathbf{r}_j)} \rangle_{\mathrm{chain}} = z t^{fN-2} \frac{fN}{2} g(q) \tag{A6}$$

$$g(q) = 1 + \frac{Nf}{1 + q^2 b^2 N/12} \tag{A7}$$

where we have introduced the correlation function of

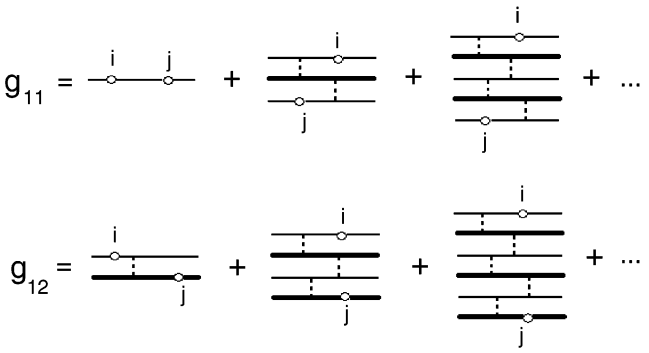

Figure 6. Diagrammatic representations of eqs A10 and A13.

one homopolymer chain $g(q)$. Note that the two labeled points are free; that is they have no diagrams attached to them. Although in principle it is possible to obtain an exact expression for $g(q)$, for our numerical analysis the interpolation given in (A7) will suffice. Note that one cannot use the Debye function for $g(q)$, since it does not provide a correct limit of point ions at $q \to \infty$.

Also we need to introduce a closely related to Σ_g sum of all diagrams where the two labels cannot belong to the same monomer

$$\Sigma_h(q) = z t^{fN-2} \frac{1}{2} \sum_{i \neq j} \langle e^{i\mathbf{q}(\mathbf{r}_i - \mathbf{r}_j)} \rangle_{\text{chain}} = z t^{fN-2} \frac{fN}{2} h(q) \quad \text{(A8)}$$

$$h(q) = g(q) - 1 = \frac{Nf}{1 + q^2 b^2 N/12} \quad \text{(A9)}$$

Since the system is symmetric we need to calculate only two functions $g_{11} = g_{22}$ and $g_{12} = g_{21}$. Using definitions A5−A9, the autocorrelation function $g_{11}(q)$ can be written as the following series

$$g_{11}(q) = t^2 \Sigma_g + t^2 \Sigma_g (\omega' \Sigma_h) \omega' \Sigma_g + t^2 \Sigma_g (\omega' \Sigma_h)^3 \omega' \Sigma_g + \ldots \quad \text{(A10)}$$

The series is depicted schematically in Figure 6. Normal lines correspond to chains of type 1, thick lines to chains of type 2, dashed lines to cross-links between the chains. The two labeled monomers i and j (the labels in the definition of $g_{\alpha\beta}(q)$ given by eq A4) are shown as empty circles. Each diagram represents a summation over all possible positions of cross-links (note that one monomeric unit cannot participate in more than one cross-link), and also over all positions of labels i and j. By construction, i and j mark the outermost chains, and in the summation, they are restricted to move only along the respective chains they label.

The first term in eq A10 is the sum of all diagrams in which the two labels belong to the same chain, which is simply $\Sigma_g(q)$ defined by eq A6. The following terms result from summation of all diagrams with labels belonging to different chains. In our model, only oppositely charged chains can associate with each other. The second term is the sum of all diagrams in which the two labels (marking monomers on chains of type 1) are separated by a chain of opposite charge (type 2). The next term in (A10) comes from summation of all diagrams with the insert between the labeled chain comprised of three chains (sequence 2−1−2). Higher terms correspond to summation of diagrams with a higher number of chains in the insert between the labeled chains.

In (A10), we introduced the effective statistical weight of the cross-link

$$\omega' = \omega e^{-q^2 b^2/6} \quad \text{(A11)}$$

which takes into account the correlations of monomers in a cross-link, which we assume to be Gaussian (b is the bond length). Note that since one monomer can form only one cross-link the presence in a diagram of a chain connecting the two labeled chains corresponds in eq A10 to a generating function Σ_h, in which summation runs over $i \neq j$. It is easy to see that the term in (A10) corresponding to the sum of all diagrams separated by $2n - 1$ chains reads $t^2 \Sigma_g (\omega' \Sigma_h)^{2n-1} \omega' \Sigma_g$. It is easy to sum the infinite series (A10) as

$$g_{11}(q) = t^2 \Sigma_g \frac{1 + \omega' \Sigma_g \omega' (\Sigma_g - \Sigma_h)}{1 - (\omega' \Sigma_h)^2} \quad \text{(A12)}$$

Analogously, for $g_{12}(q)$, we obtain

$$g_{12}(q) = t^2 \Sigma_g \omega' \Sigma_g + t^2 \Sigma_g (\omega' \Sigma_h)^2 \omega' \Sigma_g + t^2 \Sigma_g (\omega' \Sigma_h)^4 \omega' \Sigma_g + \ldots \quad \text{(A13)}$$

where the first term corresponds to all diagram with the labels belonging to two neighboring chains (of opposite charge), the next term—all diagrams with two chains separating the labeled chains and so on. Diagrammatic representation of eq A10 is also shown in Figure 6. The series in (A13) can be summed as

$$g_{12}(q) = t^2 \Sigma_g \frac{\omega' \Sigma_g}{1 - (\omega' \Sigma_h)^2} \quad \text{(A14)}$$

To use the correlators A12 and A14 in the free energy, we need to change from the variables z and t to the number concentration of charged monomers ρ_1 (for our case $\rho_1 = \rho_2$) and conversion Γ. Conversion Γ is defined as the fraction of charged monomers in cross-links

$$\Gamma = \frac{\rho^{(2)}}{\rho_1} = \frac{\rho^{(2)}}{\rho_2} \quad \text{(A15)}$$

where $\rho^{(2)}$ is the number of cross-links. As is shown in refs 23 and 24 the concentrations are given by

$$\rho_1 = \frac{z t^{fN}}{2} fN \quad \text{(A16)}$$

$$\rho^{(2)} = \omega \left(\frac{1}{2} z f N t^{fN-1} \right)^2 \quad \text{(A17)}$$

Combining it with (A5) and (A6), we obtain

$$t^2 \Sigma_g = \rho_1 g(q) \quad \text{(A18)}$$

$$\omega' \Sigma_h = \Gamma e^{-q^2 b^2/6} h(k) = \Gamma' h(k) \quad \text{(A19)}$$

which substituted into (A12) and (A14) yields

$$g_{11}(q) = \rho_1 g(q) \frac{1 + (\Gamma')^2 h(q)}{1 - [\Gamma' h(q)]^2} \quad \text{(A20)}$$

$$g_{12}(q) = \rho_1 g(q) \frac{\Gamma' g(q)}{1 - [\Gamma' h(q)]^2} \quad \text{(A21)}$$

Note that in (A19) we introduced the effective conversion Γ', which takes into account the correlations of ions in the cross-link. The divergence of the correlators at $\Gamma' h(q = 0) = 1$, i.e., $\Gamma(fN - 1) = 1$ corresponds to gelation.[23,24,51]

The value of Γ can be obtained from the definition of Γ (given by eq A15) using relations A5, A16, and A17. Conversion turns out to be determined by the unmodified mass action law

$$\frac{\Gamma}{(1-\Gamma)^2} = \rho_1 \omega = \rho_1 e^{\epsilon} \qquad \text{(A22)}$$

This reflects the fact that in this Appendix we considered an ideal associating system (no other interactions except association are present). Conversion for the solution of associating polyelectrolytes is obtained from the minimization of the total free energy, which includes interaction terms. The resulting modified mass action law (eq 28) differs from eq A22 in that it has a long-range electrostatic contribution to the effective binding energy.

References and Notes

(1) Bloomfield, V. A. *Curr. Opin. Struct. Biol.* **1996**, *6*, 334.
(2) Raspaud, E.; Olvera de la Cruz, M.; Sikorav, J.-L.; Livolant, F. *Biophys. J.* **1998**, *74*, 381. Raspaud, E.; Chaperon, I.; Leforestier, A.; Livolant, F. *Biophys. J.* **1999**, *77*, 1547.
(3) Levin, Y. *Rep. Prog. Phys.* **2002**, *65*, 1577.
(4) Izumrudov, V.; Zezin, A.; Kabanov, V. *Usp. Khim.* **1991**, *60*, 1570.
(5) Decher, G. *Science* **1997**, *277*, 1232.
(6) Messina, R. *Macromolecules* **2004**, *37*, 621.
(7) Leclercq, L.; Boustta, M.; Vert, M. *J. Drug Target.* **2003**, *11*, 129.
(8) Nystrom, R.; Hedstrom, G.; Gustafsson, J.; Rosenholm, J. B. *Colloids Surf. A* **2004**, *234*, 85.
(9) Mende, M.; Petzold, G.; Buchhammer, H.-M. *Colloid Polym. Sci.* **2002**, *280*, 342.
(10) Kabanov, V. A. In *Macromolecular Complexes in Chemistry and Biology;* Dubin, P., et al., Eds.; Springer: New York, 1994.
(11) Philipp, B.; Dautzenberg, H.; Linow, K. J.; Kotz, J.; Dawydoff, W. *Prog. Polym. Sci.* **1998**, *14*, 823.
(12) Dautzenberg, H. *Macromol. Symp.* **2000**, *162*, 1.
(13) Tsuchida, E. *J. Macromol. Sci.—Pure Appl. Chem.* **1994**, *A31*, 1.
(14) Pogodina, N. V.; Tsvetkov, N. V. *Macromolecules* **1997**, *30*, 4897.
(15) Borue, V. Yu.; Erukhimovich, I. Ya. *Macromolecules* **1990**, *23*, 3625.
(16) Castelnovo, M.; Joanny, J.-F. *Eur. Phys. J. E* **2001**, *6*, 377.
(17) Castelnovo, M.; Joanny, J.-F. *Macromolecules* **2002**, *35*, 4531.
(18) Kudlay, A.; Olvera de la Cruz, M. *J. Chem. Phys.* **2004**, *120*, 404.
(19) Biesheuvel, P. M.; Cohen Stuart, M. A. *Langmuir* **2004**, *20*, 2785.
(20) Manning, G. S. *J. Chem. Phys.* **1969**, *51*, 924.
(21) Dobrynin, A. V.; Rubinstein, M. *Macromolecules* **2001**, *34*, 1964.
(22) Joanny, J.-F. *Polymer* **1980**, *21*, 71.
(23) Ermoshkin, A. V.; Erukhimovich, I. Ya. *J. Chem. Phys.* **1999**, *110*, 1781.
(24) Ermoshkin, A. V.; Kudlay, A.; Olvera de la Cruz, M. *J. Chem. Phys.* **2004**, *120*, 11930.
(25) Dobrynin, A. V. *Macromolecules* **2004**, *37*, 3881.
(26) Park, S. Y.; Barrett, C. J.; Rubner, M. F.; Mayes, A. M. *Macromolecules* **2001**, *34*, 3384.
(27) Sukhishvili, S.; Granick, S. *J. Chem. Phys.* **1998**, *109*, 6861.
(28) Park, S. Y.; Rubner, M. F.; Mayes, A. M. *Langmuir* **2002**, *18*, 9600.
(29) Borue, V. Yu.; Erukhimovich, I. Ya. *Macromolecules* **1988**, *21*, 3240.
(30) Joanny, J.-F.; Leibler, L. *J. Phys. (Paris)* **1990**, *51*, 545.
(31) Khokhlov, A. R.; Khachaturian, K. A. *Polymer* **1982**, *23*, 1743.
(32) Dobrynin, A. V.; Colby, R. H.; Rubinstein, M. *Macromolecules* **1995**, *28*, 1859.
(33) Semenov, A. N.; Rubinstein, M. *Macromolecules* **1998**, *31*, 1373.
(34) Khokhlov, A. R.; Nyrkova, I. A. *Macromolecules* **1992**, *25*, 1493.
(35) Yerukhimovich, I. Ya. *Polym. Sci. USSR* **1979**, *21*, 470. Yerukhimovich, I. Ya. *Polym. Sci. USSR* **1982**, *24*, 2223.
(36) de Gennes, P.-G. *Scaling Concepts in Polymer Physics*; Cornell University Press: Ithaca, NY, 1979.
(37) Benoit, H. C.; Higgins, J. S. *Polymers and Neutron Scattering*; Oxford University Press: New York, 1996.
(38) Ermoshkin, A. V.; Olvera de la Cruz, M. *Macromolecules* **2003**, *36*, 7824.
(39) Kudlay, A.; Ermoshkin, A. V.; Olvera de la Cruz, M. *Phys. Rev. E.* **2004**, *70*, 021504.
(40) Gonzalez-Mozuelos, P.; Olvera de la Cruz, M. *J. Chem. Phys.* **2003**, *118*, 4684.
(41) Dobrynin, A. V.; Rubinstein, M.; Obukhov, S. P. *Macromolecules* **1996**, *29*, 2974.
(42) Kabanov, V. In *Multilayer Thin Films: Sequential Assembly of Nanocomposite Materials*; Decher, G., Schlenoff, J. B., Eds.; Wiley-VCH: Weinheim, Germany, 2003.
(43) Dautzenberg, H. *Macromolecules* **1997**, *30*, 7810.
(44) Dautzenberg, H.; Karibyants, N. *Macromol. Chem. Phys.* **1998**, *200*, 118.
(45) Dautzenberg, H.; Jaeger, W. *Macromol. Chem. Phys.* **2002**, *202*, 2095.
(46) Dautzenberg, H.; Rother, G. *Macromol. Chem. Phys.* **2004**, *205*, 114.
(47) Solis, F. J.; Olvera de la Cruz, M. *J. Chem. Phys.* **2000**, *112*, 2030.
(48) Solis, F. J.; Olvera de la Cruz, M. *Eur. Phys. J. E* **2001**, *4*, 143.
(49) Erukhimovich, I. Y. *JETP* **1995**, *81*, 553.
(50) Ermoshkin, A. V.; Olvera de la Cruz, M. *J. Polym. Sci., Polym. Phys.* **2004**, *42*, 766.
(51) Ermoshkin, A. V.; Olvera de la Cruz, M. *Phys. Rev. Lett.* **2003**, *90*, 125504.

MA048519T